Progress In Electromagnetics Research, PIER 22, 293–313, 1999

STATISTICAL NON-GAUSSIAN MODEL OF SEA SURFACE WITH ANISOTROPIC SPECTRUM FOR WAVE SCATTERING THEORY. PART II

V. I. Tatarskii and V. V. Tatarskii

University of Colorado/CIRES and
NOAA/ERL/Environmental Technology Laboratory
325 Broadway, Boulder, Colorado

10. A SCATTERING CROSS SECTION FROM THE ABSOLUTELY REFLECTING INTERFACE IN THE KIRCHHOFF APPROXIMATION

For a scattering cross section $\Sigma(\mathbf{q}, \mathbf{q}_0)$ for both the Dirichlet and Neuman cases (in the Kirchhoff approximation these two cases coincide), we have[11] (see, e.g., [1]):

[11] Formulae numeration in Part II of the paper is a continuation of the numeration in Part I.

$$\Sigma\left(\mathbf{q},\mathbf{q}_0\right)=4\pi^2\left[\frac{k^2+\nu\nu_0-\mathbf{q}\mathbf{q}_0}{\nu+\nu_0}\right]^2\left\langle\left|\mathcal{J}\left(\mathbf{q}-\mathbf{q}_0,\nu+\nu_0\right)\right|^2\right\rangle. \quad (118)$$

Here, the wave vector of the incident plane wave $\mathbf{k}_0=\left(\mathbf{q}_0,-\nu_0\right)$ has the horizontal component $\mathbf{q}_0$ and the vertical component $\nu_0=\sqrt{k^2-\mathbf{q}_0^2}$, and the wave vector of the scattered wave has the form $\mathbf{k}=(\mathbf{q},\nu)$, where $\nu=\sqrt{k^2-\mathbf{q}^2}$. The value $\left\langle\left|\mathcal{J}\right|^2\right\rangle$ is given by the formula

$$\begin{aligned}\left\langle\left|\mathcal{J}\left(\mathbf{q}-\mathbf{q}_0,\nu+\nu_0\right)\right|^2\right\rangle=&\frac{1}{16\pi^4}\iint d^2r'\iint d^2r''\exp\left[i\left(\mathbf{q}-\mathbf{q}_0\right)\left(\mathbf{r}'-\mathbf{r}''\right)\right]\\&\times\left\langle\exp\left\{i\left(\nu+\nu_0\right)\left[\zeta\left(\mathbf{r}'\right)-\zeta\left(\mathbf{r}''\right)\right]\right\}\right\rangle\end{aligned} \quad (119)$$

The mean value appearing in this formula,

$$\left\langle\exp\left\{i\left(\nu+\nu_0\right)\left[\zeta\left(\mathbf{r}'\right)-\zeta\left(\mathbf{r}''\right)\right]\right\}\right\rangle,$$

is the CF for the differences in elevation that can be expressed in terms of (87):

$$\begin{aligned}&\left\langle\exp\left\{i\left(\nu+\nu_0\right)\left[\zeta\left(\mathbf{r}'\right)-\zeta\left(\mathbf{r}''\right)\right]\right\}\right\rangle\\&\quad\approx\sum_\mu P_\mu\exp\left\{i\left(\nu+\nu_0\right)\mathcal{L}\left(\mathbf{r}',\mathbf{r}''\right)\right.\\&\qquad\left.-\frac{1}{2}\left(\nu+\nu_0\right)^2\left\{\lambda_\mu D\left(\mathbf{r}''-\mathbf{r}'\right)-\left[\mathcal{L}\left(\mathbf{r}',\mathbf{r}''\right)\right]^2\right\}\right\}.\end{aligned} \quad (120)$$

Here,

$$\mathbf{r}'=\left(x',y'\right),\ \mathbf{r}''=\left(x'',y''\right),\ l_1=x''-x',\ l_2=y''-y',\ \mathbf{r}''-\mathbf{r}'=(l_1,l_2), \quad (121)$$

and

$$\mathbf{m}_1 l_1\left(\mathbf{r}',\mathbf{r}''\right)=(l_1,0),\ \mathbf{m}_2 l_2\left(\mathbf{r}',\mathbf{r}''\right)=(0,l_2). \quad (122)$$

For (119) we obtain, choosing

$$\mathbf{r}'\text{ and }\mathbf{r}''-\mathbf{r}'\equiv\mathbf{r}=(l_1,l_2)$$

as new variables of integration:

$$\left\langle \left|\mathcal{J}\left(\mathbf{q}-\mathbf{q}_0,\nu+\nu_0\right)\right|^2\right\rangle$$
$$=\frac{1}{16\pi^4}\sum_{\mu}P_{\mu}\iint d^2r'\int dl_1\int dl_2\exp\left[i\left(q_1-q_{10}\right)l_1+i\left(q_2-q_{20}\right)l_2\right]$$
$$\times\exp\left\{i\left(\nu+\nu_0\right)\widetilde{\mathcal{L}}\left(l_1,l_2\right)-\frac{1}{2}\left(\nu+\nu_0\right)^2\left\{\lambda_{\mu}D\left(l_1,l_2\right)-\left[\widetilde{\mathcal{L}}\left(l_1,l_2\right)\right]^2\right\}\right\}; \tag{123}$$

where we denoted the value $\mathcal{L}$ depending on new variables l_1 and l_2 as $\widetilde{\mathcal{L}}\left(l_1,l_2\right)$:

$$\widetilde{\mathcal{L}}\left(l_1,l_2\right)\equiv\kappa_{1,\mu}l_1\sqrt{\frac{D\left(l_1,0\right)}{l_1^2}}-\kappa_{2,\mu}l_2\sqrt{\frac{D\left(0,l_2\right)}{l_2^2}}. \tag{124}$$

Taking into account that

$$\iint d^2r'=A,$$

where $A\to\infty$ is the total scattering area, we obtain

$$\frac{1}{A}\left\langle \left|\mathcal{J}\left(\mathbf{q}-\mathbf{q}_0,\nu+\nu_0\right)\right|^2\right\rangle$$
$$=\frac{1}{16\pi^4}\sum_{\mu}P_{\mu}\int dl_1\int dl_2$$
$$\times\exp\left\{i\left(q_1-q_{10}\right)l_1+i\left(q_2-q_{20}\right)l_2+i\left(\nu+\nu_0\right)\widetilde{\mathcal{L}}\left(l_1,l_2\right)\right.$$
$$\left.-\frac{1}{2}\left(\nu+\nu_0\right)^2\left\{\lambda_{\mu}D\left(l_1,l_2\right)-\left[\widetilde{\mathcal{L}}\left(l_1,l_2\right)\right]^2\right\}\right\}. \tag{125}$$

For the scattering cross section from the unit of area, $\Sigma_0\equiv\Sigma/A$, we obtain

$$\Sigma_0\left(\mathbf{q},\mathbf{q}_0\right)$$
$$=\left[\frac{k^2+\nu\nu_0-\mathbf{q}\mathbf{q}_0}{2\pi\left(\nu+\nu_0\right)}\right]^2\sum_{\mu}P_{\mu}\int dl_1\int dl_2\exp\left[i\left(q_1-q_{10}\right)l_1+i\left(q_2-q_{20}\right)l_2\right]$$
$$\times\exp\left\{i\left(\nu+\nu_0\right)\widetilde{\mathcal{L}}\left(l_1,l_2\right)-\frac{1}{2}\left(\nu+\nu_0\right)^2\left\{\lambda_{\mu}D\left(l_1,l_2\right)-\left[\widetilde{\mathcal{L}}\left(l_1,l_2\right)\right]^2\right\}\right\} \tag{126}$$

The function $D(\mathbf{r})$ saturates while $r \to \infty$, and $D(\infty) = 2\sigma_0^2$, where $\sigma_0^2 = \langle \zeta^2 \rangle$ is the rms. of the surface elevations. Because of this, it is useful to separate the singular integrals in (126).

Let us denote

$$\mathcal{F}(l_1, l_2) = \frac{1}{2}(\nu + \nu_0)^2 \left\{ \lambda_\mu D(l_1, l_2) - \left[\widetilde{\mathcal{L}}(l_1, l_2) \right]^2 \right\}. \tag{127}$$

In terms of $\mathcal{F}(l_1, l_2)$ (126) takes the form

$$\begin{aligned} \Sigma_0(\mathbf{q}, \mathbf{q}_0) &= \left[\frac{k^2 + \nu\nu_0 - \mathbf{q}\mathbf{q}_0}{2\pi(\nu + \nu_0)} \right]^2 \\ &\times \sum_\mu P_\mu \int dl_1 \int dl_2 \exp\left\{ i\left[(q_1 - q_{10}) l_1 + (q_2 - q_{20}) l_2 \right] + i(\nu + \nu_0) \widetilde{\mathcal{L}}(l_1, l_2) \right\} \\ &\times \exp\left[-\mathcal{F}(l_1, l_2) \right]. \end{aligned} \tag{128}$$

We present $\exp[-\mathcal{F}(l_1, l_2)]$ in the form

$$\exp\left[-\mathcal{F}(l_1, l_2) \right] = A(l_1, l_2) + B(l_1, l_2), \tag{129}$$

where

$$\begin{aligned} A(l_1, l_2) \equiv \exp\left[-\mathcal{F}(l_1, l_2) \right] - \exp\left[-\mathcal{F}(l_1, \infty) \right] \\ - \exp\left[-\mathcal{F}(\infty, l_2) \right] + \exp\left[-\mathcal{F}(\infty, \infty) \right], \end{aligned} \tag{130}$$

and

$$B(l_1, l_2) = \exp\left[-\mathcal{F}(l_1, \infty) \right] + \exp\left[-\mathcal{F}(\infty, l_2) \right] - \exp\left[-\mathcal{F}(\infty, \infty) \right]. \tag{131}$$

The function $A(l_1, l_2)$ satisfies the conditions

$$A(\infty, l_2) = A(l_1, \infty) = A(\infty, \infty) = 0. \tag{132}$$

Thus, if we substitute in (128) the sum (129) instead of $\exp(-\mathcal{F})$, the term containing A will converge. The second term containing B leads to the sum of δ-functions and contributes only to the specular directions. Thus, the diffuse part of the scattering cross section is given by the formula

$$\begin{aligned} \Sigma_0 &= \left[\frac{k^2 + \nu\nu_0 - \mathbf{q}\mathbf{q}_0}{2\pi(\nu + \nu_0)} \right]^2 \\ &\times \sum_\mu P_\mu \int dl_1 \int dl_2 \exp\left[i(q_1 - q_{10}) l_1 + i(q_2 - q_{20}) l_2 \right] A(l_1, l_2). \end{aligned} \tag{133}$$

From (127) we obtain

$$\mathcal{F}(l_1,\pm\infty)=\frac{1}{2}(\nu+\nu_0)^2\left\{2\lambda_\mu\sigma_0^2-\left[\kappa_{1,\mu}\frac{l_1}{|l_1|}\sqrt{D(l_1,0)}\mp\kappa_{2,\mu}\sigma_0\sqrt{2}\right]^2\right\}, \tag{134}$$

$$\mathcal{F}(\pm\infty,l_2)=\frac{1}{2}(\nu+\nu_0)^2\left\{2\lambda_\mu\sigma_0^2-\left[\pm\kappa_{1,\mu}\sigma_0\sqrt{2}-\kappa_{2,\mu}\frac{l_2}{|l_2|}\sqrt{D(0,l_2)}\right]^2\right\}, \tag{135}$$

$$\mathcal{F}\left(\pm\infty,\pm\infty'\right)=(\nu+\nu_0)^2\left[\lambda_\mu-\left(\pm\kappa_{1,\mu}-\left(\pm'\right)\kappa_{2,\mu}\right)^2\right]\sigma_0^2. \tag{136}$$

These formulae were used in our numerical calculations.[12]

10.1 Geometric Optics Limit

The geometric optics (GO) limit corresponds to the expansion of the function

$$F(l_1,l_2)\equiv i(\nu+\nu_0)\,\widetilde{\mathcal{L}}(l_1,l_2)-\mathcal{F}(l_1,l_2)$$

in powers of l_1 and l_2 and keeping the terms up to the second order in this expansion. Because l_1 and l_2 correspond to the principal directions, the cross-term l_1l_2 does not appear in this expansion. Using (95), we obtain

$$D(l_1,l_2)=a_1l_1^2+a_2l_2^2+O\left(l^4\right).$$

It follows from (61) that $a_1=\left\langle\gamma_1^2\right\rangle$ and $a_2=\left\langle\gamma_2^2\right\rangle$:

$$D(l_1,l_2)=\left\langle\gamma_1^2\right\rangle l_1^2+\left\langle\gamma_2^2\right\rangle l_2^2+O\left(l^4\right). \tag{137}$$

Thus, the expansion of the function F after combining similar terms has the form

$$\begin{aligned}F(l_1,l_2)\approx F_0(l_1,l_2)\equiv{}& i(\nu+\nu_0)\left[\kappa_{1,\mu}l_1\sqrt{\left\langle\gamma_1^2\right\rangle}-\kappa_{2,\mu}l_2\sqrt{\left\langle\gamma_2^2\right\rangle}\right]\\ &-\frac{1}{2}(\nu+\nu_0)^2\left\{\left(\lambda_\mu-\kappa_{1,\mu}^2\right)\left\langle\gamma_1^2\right\rangle l_1^2+\left(\lambda_\mu-\kappa_{2,\mu}^2\right)\left\langle\gamma_2^2\right\rangle l_2^2\right.\\ &\left.+2\kappa_{1,\mu}\kappa_{2,\mu}\sqrt{\left\langle\gamma_1^2\right\rangle\left\langle\gamma_2^2\right\rangle}l_1l_2\right\}.\end{aligned} \tag{138}$$

[12] The additional restriction for the parameters λ_μ, $\kappa_{1\mu}$, and $\kappa_{2\mu}$ appears from (136): $\lambda_\mu\geq(\kappa_{1\mu}\pm\kappa_{2\mu})^2$. This restriction differs from (72).

Let us compare the formula (138) with the formula (97) for the joint CF of two principal slopes. This CF has the form

$$\langle \exp\left[i\alpha\left(l_1\gamma_1 + l_2\gamma_2\right)\right]\rangle = \Theta_{\gamma_1,\gamma_2}\left(\alpha l_1, \alpha l_2\right) \approx \sum_{\mu} P_\mu \Theta_{\mu;\gamma_1,\gamma_2}\left(\alpha l_1, \alpha l_2\right)$$

where $\Theta_{\mu;\gamma_1,\gamma_2}\left(\alpha l_1, \alpha l_2\right)$ is the conditional CF:

$$\begin{aligned}\Theta_{\mu;\gamma_1,\gamma_2}\left(\alpha l_1, \alpha l_2\right) = \exp\Bigg\{ & i\alpha\left[\kappa_{1,\mu} l_1 \sqrt{\left\langle \gamma_1^2\right\rangle} - \kappa_{2,\mu} l_2 \sqrt{\left\langle \gamma_2^2\right\rangle}\right] \\ & - \frac{1}{2}\alpha^2\left\{\lambda_\mu\left[l_1^2\left\langle \gamma_1^2\right\rangle + l_2^2\left\langle \gamma_2^2\right\rangle\right]\right. \\ & \left. - \left[\kappa_{1,\mu} l_1 \sqrt{\left\langle \gamma_1^2\right\rangle} - \kappa_{2,\mu} l_2 \sqrt{\left\langle \gamma_2^2\right\rangle}\right]^2\right\}\Bigg\}.\end{aligned} \tag{139}$$

From comparison of (138) and (139) we see that

$$\exp\left[F_0\left(l_1, l_2\right)\right] = \Theta_{\mu;\gamma_1,\gamma_2}\left(\left(\nu + \nu_0\right) l_1, \left(\nu + \nu_0\right) l_2\right). \tag{140}$$

Let us substitute (140) in (128). We obtain

$$\begin{aligned}\Sigma_0 = & \left[\frac{k^2 + \nu\nu_0 - \mathbf{q}\mathbf{q}_0}{2\pi\left(\nu + \nu_0\right)}\right]^2 \sum_{\mu} P_\mu \int dl_1 \int dl_2 \\ & \times \exp\left[i\left(q_1 - q_{10}\right) l_1 + i\left(q_2 - q_{20}\right) l_2\right] \Theta_{\mu;\gamma_1,\gamma_2}\left(\left(\nu + \nu_0\right) l_1, \left(\nu + \nu_0\right) l_2\right).\end{aligned} \tag{141}$$

If we change the variables of integration according to the formula

$$\left(\nu + \nu_0\right) l_1 = \beta_1,\ \left(\nu + \nu_0\right) l_2 = \beta_2;\ dl_1 dl_2 = \frac{d\beta_1 d\beta_2}{\left(\nu + \nu_0\right)^2},$$

we obtain

$$\begin{aligned}\Sigma_0 = & \frac{\left(k^2 + \nu\nu_0 - \mathbf{q}\mathbf{q}_0\right)^2}{4\pi^2\left(\nu + \nu_0\right)^4} \sum_{\mu} P_\mu \int d\beta_1 \int d\beta_2 \Theta_{\mu;\gamma_1,\gamma_2}\left(\beta_1, \beta_2\right) \\ & \times \exp\left[i\frac{q_1 - q_{10}}{\nu + \nu_0}\beta_1 + i\frac{q_2 - q_{20}}{\nu + \nu_0}\beta_2\right].\end{aligned} \tag{142}$$

But, according to definition,

$$\frac{1}{4\pi^2}\iint \exp\left(-i\beta_1\gamma_1 - i\beta_2\gamma_2\right) \Theta_{\mu;\gamma_1,\gamma_2}\left(\beta_1, \beta_2\right) d\beta_1 d\beta_2 = W_{\mu,\gamma_1,\gamma_2}\left(\gamma_1, \gamma_2\right) \tag{143}$$

is the joint conditional PDF of two principal slopes. Thus, (142) takes the form

$$\Sigma_0 = \frac{\left(k^2 + \nu\nu_0 - \mathbf{q}\mathbf{q}_0\right)^2}{\left(\nu + \nu_0\right)^4} \sum_{\mu} P_\mu W_{\mu,\gamma_1,\gamma_2} \left(\frac{q_{10} - q_1}{\nu + \nu_0}, \frac{q_{20} - q_2}{\nu + \nu_0} \right). \quad (144)$$

The sum on the right-hand side is equal to the initial joint PDF of two principal slopes. Thus, we can finally write the formula

$$\Sigma_0 = \frac{\left(k^2 + \nu\nu_0 - \mathbf{q}\mathbf{q}_0\right)^2}{\left(\nu + \nu_0\right)^4} W_{\gamma_1,\gamma_2} \left(\frac{q_{10} - q_1}{\nu + \nu_0}, \frac{q_{20} - q_2}{\nu + \nu_0} \right). \quad (145)$$

The function $W_{\mu,\gamma_1,\gamma_2}(\gamma_1, \gamma_2)$ was obtained above (see (71)):

$$\begin{aligned} W_\gamma(\gamma_1, \gamma_2) = \sum_{\mu} & \frac{P_\mu}{2\pi\sqrt{\lambda_\mu \left(\lambda_\mu - \kappa_{1,\mu}^2 - \kappa_{2,\mu}^2\right) \left\langle \gamma_1^2 \right\rangle \left\langle \gamma_2^2 \right\rangle}} \\ & \times \exp\left\{ - \frac{\left(\lambda_\mu - \kappa_{2,\mu}^2\right) \left[\gamma_1 - \kappa_{1,\mu}\sqrt{\left\langle \gamma_1^2 \right\rangle}\right]^2}{2\left\langle \gamma_1^2 \right\rangle \lambda_\mu \left(\lambda_\mu - \kappa_{1,\mu}^2 - \kappa_{2,\mu}^2\right)} \right. \\ & - \frac{\left(\lambda_\mu - \kappa_{1,\mu}^2\right) \left[\gamma_2 - \kappa_{2,\mu}\sqrt{\left\langle \gamma_2^2 \right\rangle}\right]^2}{2\left\langle \gamma_2^2 \right\rangle \lambda_\mu \left(\lambda_\mu - \kappa_{1,\mu}^2 - \kappa_{2,\mu}^2\right)} \\ & \left. - \frac{\kappa_{1,\mu}\kappa_{2,\mu} \left[\gamma_1 - \kappa_{1,\mu}\sqrt{\left\langle \gamma_1^2 \right\rangle}\right] \left[\gamma_2 - \kappa_{2,\mu}\sqrt{\left\langle \gamma_2^2 \right\rangle}\right]}{\sqrt{\left\langle \gamma_1^2 \right\rangle \left\langle \gamma_2^2 \right\rangle} \lambda_\mu \left(\lambda_\mu - \kappa_{1,\mu}^2 - \kappa_{2,\mu}^2\right)} \right\}. \end{aligned}$$

10.2 General Approach to Geometric Optics Approximation

We show in this subsection that the formula (145) obtained by using decomposition of the PDF in the sum of Gaussian terms has a universal meaning (since this is a well-known fact, we include the following derivation only for completeness of the paper). We start with the formula

$$\Sigma(\mathbf{q}, \mathbf{q}_0) = 4\pi^2 \left[\frac{k^2 + \nu\nu_0 - \mathbf{q}\mathbf{q}_0}{\nu + \nu_0} \right]^2 \left\langle \left| \mathcal{J}(\mathbf{q} - \mathbf{q}_0, \nu + \nu_0) \right|^2 \right\rangle,$$

where

$$\left\langle \left|\mathcal{J}\left(\mathbf{q}-\mathbf{q}_0,\nu+\nu_0\right)\right|^2\right\rangle = \frac{1}{16\pi^4}\iint d^2r' \iint d^2r'' \times \exp\left[i\left(\mathbf{q}-\mathbf{q}_0\right)\left(\mathbf{r}'-\mathbf{r}''\right)\right]\left\langle \exp\left\{i\left(\nu+\nu_0\right)\left[\zeta\left(\mathbf{r}'\right)-\zeta\left(\mathbf{r}''\right)\right]\right\}\right\rangle .$$

In the GO limit we expand the difference $\zeta\left(\mathbf{r}'\right)-\zeta\left(\mathbf{r}''\right)$ as follows:

$$\begin{aligned} &\mathbf{r}'=\mathbf{r}+\frac{\rho}{2}; \qquad \mathbf{r}''=\mathbf{r}-\frac{\rho}{2}; \qquad \zeta\left(\mathbf{r}'\right)=\zeta\left(\mathbf{r}\right)+\frac{\rho}{2}\nabla\zeta\left(\mathbf{r}\right); \\ &\zeta\left(\mathbf{r}''\right)=\zeta\left(\mathbf{r}\right)-\frac{\rho}{2}\nabla\zeta\left(\mathbf{r}\right); \qquad \zeta\left(\mathbf{r}'\right)-\zeta\left(\mathbf{r}''\right)=\rho\nabla\zeta\left(\mathbf{r}\right)=\rho\gamma, \end{aligned} \tag{146}$$

where $\gamma=\nabla\zeta\left(\mathbf{r}\right)$. Then,

$$\begin{aligned} &\left\langle \left|\mathcal{J}\left(\mathbf{q}-\mathbf{q}_0,\nu+\nu_0\right)\right|^2\right\rangle \\ &\quad=\frac{1}{16\pi^4}\iint d^2r \iint d^2\rho \exp\left[i\left(\mathbf{q}-\mathbf{q}_0\right)\rho\right]\left\langle \exp\left\{i\left(\nu+\nu_0\right)\rho\gamma\right\}\right\rangle \\ &\quad=\frac{A}{16\pi^4}\iint d^2\rho \exp\left[i\left(\mathbf{q}-\mathbf{q}_0\right)\rho\right]\left\langle \exp\left\{i\left(\nu+\nu_0\right)\rho\gamma\right\}\right\rangle , \end{aligned} \tag{147}$$

where A is the total scattering area. For the last exponential we have

$$\left\langle \exp\left\{i\left(\nu+\nu_0\right)\rho\gamma\right\}\right\rangle = \iint \exp\left\{i\left(\nu+\nu_0\right)\rho\gamma\right\} W_\gamma\left(\gamma\right) d^2\gamma, \tag{148}$$

and substituting (148) in (147) we obtain

$$\begin{aligned} &\left\langle \left|\mathcal{J}\left(\mathbf{q}-\mathbf{q}_0,\nu+\nu_0\right)\right|^2\right\rangle \\ &\quad=\frac{A}{16\pi^4}\iint d^2\rho \exp\left[i\left(\mathbf{q}-\mathbf{q}_0\right)\rho\right]\iint \exp\left\{i\left(\nu+\nu_0\right)\rho\gamma\right\} W_\gamma\left(\gamma\right) d^2\gamma \\ &\quad=\frac{A}{16\pi^4}\iint W_\gamma\left(\gamma\right) d^2\gamma \iint d^2\rho \exp\left[i\left(\mathbf{q}-\mathbf{q}_0+\left(\nu+\nu_0\right)\gamma\right)\rho\right]. \end{aligned} \tag{149}$$

Because the last integral over ρ presents the 2-D δ-function, using the known formula $\delta_2\left(a\mathbf{x}\right)=\left|a\right|^{-2}\delta_2\left(\mathbf{x}\right)$, we obtain

$$\left\langle \left|\mathcal{J}\left(\mathbf{q}-\mathbf{q}_0,\nu+\nu_0\right)\right|^2\right\rangle = \frac{A}{4\pi^2\left(\nu+\nu_0\right)^2} W_\gamma\left(\frac{\mathbf{q}_0-\mathbf{q}}{\nu+\nu_0}\right).$$

Thus,

$$\Sigma_{0,\text{geom}} = \frac{\left(k^2 + \nu\nu_0 - \mathbf{q}\mathbf{q}_0\right)^2}{\left(\nu + \nu_0\right)^4} W_\gamma \left(\frac{\mathbf{q}_0 - \mathbf{q}}{\nu_0 + \nu}\right). \tag{150}$$

According to this formula, in the GO limit the scattering cross section is proportional to the PDF of slopes of a surface satisfying the specular reflection condition. This result has a simple physical meaning: the scattering cross section is proportional to the number of surface facets having the appropriate slope.

11. NUMERICAL RESULTS FOR THE RADAR CROSS SECTION FOR COX-MUNK PDF AND 2-D ANISOTROPIC SPECTRA

11.1 Determining the Parameters of the PDF

We now consider an example, the joint PDF of slopes, taken from papers [2, 3] for the wind speed $u_{10} = 10m/\sec$. We seek the parameters of approximation, $\kappa_{1,\mu}$, $\kappa_{2,\mu}$, λ_μ, and P_μ, by minimizing the integrated square of the difference between Cox and Munk function $W_{\text{CM}}(\gamma_1, \gamma_2)$ and its approximation $W_\gamma(\gamma_1, \gamma_2)$, given by the formula (71):

$$E^2 \equiv \iint \left[W_{\text{CM}}(\gamma_1, \gamma_2) - W_\gamma(\gamma_1, \gamma_2)\right]^2 d\gamma_1 d\gamma_2.$$

We used [4] "Simulated Annealing" minimization algorithm for searching the global minimum. The parameters, obtained for this example, are presented in the following table:

Table 1. Parameters of approximation of the Cox-Munk joint PDF for slopes for $u = 10m/s$

μ	P_μ	λ_μ	$\kappa_{1\mu}$	$\kappa_{2\mu}$
±1	0.2219658	1.1135315	-0.04151202	±0.4965694
±2	0.2058264	0.6431118	$+0.01032697$	±0.3410244
±3	0.0722078	1.5560527	-0.09817264	±0.7710721

The difference between the joint PDF $W_{\text{CM}}(\gamma_1, \gamma_2)$ [2] and the approximation $W_\gamma(\gamma_1, \gamma_2)$ given by (71) is presented in Figure 3. The

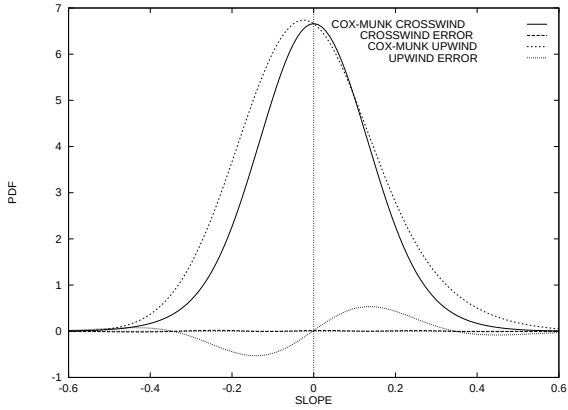

Figure 3. Approximation of the Cox-Munk upwind and cross-wind PDF for the wind speed $u_{10} = 10$ m/s and errors of approximations. Real approximation was performed for 2-D PDF, but to make the results clearer we presented only two cross sections of the 2-D PDF.

relative accuracy of this approximation,

$$\delta = \frac{\sqrt{\iint\limits_{-\infty}^{\infty}\iint\limits_{-\infty}^{\infty} \left[W_{\mathrm{CM}}\left(\gamma_1,\gamma_2\right) - W_{\gamma}\left(\gamma_1,\gamma_2\right)\right]^2 d\gamma_1 d\gamma_2}}{\sqrt{\iint\limits_{-\infty}^{\infty}\iint\limits_{-\infty}^{\infty} W_{\mathrm{CM}}^2\left(\gamma_1,\gamma_2\right) d\gamma_1 d\gamma_2}}$$

is about 7.7 %.[13]

Similar measurements made with a scanning laser slope gauge were published in [5, 6].

In applications not only the PDF is important but also the spectrum, or correlation (structure) function. In our previous paper [7] we used the generalized experimental spectrum of surface presented in [8]. But this spectrum does not agree with the PDF of slopes based on [2] data.

According to (61), the values $\left\langle \gamma_1^2 \right\rangle$, $\left\langle \gamma_2^2 \right\rangle$ can be expressed in terms of $D\left(\mathbf{r}\right)$ by the formulae

$$\left\langle \gamma_1^2 \right\rangle = \lim_{l_1 \to 0} \frac{D\left(l_1 \mathbf{m}_1\right)}{l_1^2}, \quad \left\langle \gamma_2^2 \right\rangle = \lim_{l_2 \to 0} \frac{D\left(l_2 \mathbf{m}_2\right)}{l_2^2}. \tag{151}$$

[13] We choose normalization such that the ratio is dimensionless.

Substituting the spectral representation (55),

$$D(r,\psi) = 2\iint [1-\cos(\mathbf{qr})]\,\Phi(q,\varphi)\,qdqd\varphi,$$

we find

$$\left\langle \gamma_1^2 \right\rangle = \lim_{l\to 0}\frac{2}{l^2}\int\limits_0^\infty qdq\int\limits_0^{2\pi}[1-\cos(ql\cos\varphi)]\,\Phi(q,\varphi).$$

Because

$$\lim_{l\to 0}\frac{2}{l^2}[1-\cos(ql\cos\varphi)] = \lim_{l\to 0}\frac{2}{l^2}\cdot 2\sin^2\left(\frac{ql\cos\varphi}{2}\right) = q^2\cos^2\varphi$$

we obtain

$$\int W_1(\gamma_1)\,\gamma_1^2 d\gamma_1 = \left\langle \gamma_1^2 \right\rangle = \int\limits_0^\infty q^3 dq\int\limits_0^{2\pi}\Phi(q,\varphi)\cos^2\varphi d\varphi. \qquad (152)$$

Similarly,

$$\int W_2(\gamma_2)\,\gamma_2^2 d\gamma_2 = \left\langle \gamma_2^2 \right\rangle = \int\limits_0^\infty q^3 dq\int\limits_0^{2\pi}\Phi(q,\varphi)\sin^2\varphi d\varphi. \qquad (153)$$

If we find the values $\left\langle \gamma_1^2 \right\rangle$ and $\left\langle \gamma_2^2 \right\rangle$ from the [2] data (the integrals on the left-hand sides of (152) and (153)), we obtain significant differences from the values calculated via the integrals on the right-hand sides of (152) and (153), based on [8].[14] In [10] this controversy was resolved by incorporating the slope data in the spectrum. Because of this, we used the generalized spectrum suggested in [10] in our calculations.[15]

11.2 Calculations of the Radar Cross Sections in the Kirchhoff Approximation

We used the formula (133) for calculations of the scattering cross sections. The functions entering in (133) are determined by the formulae (127), (130), (134), (135), and (161) for structure function of

[14] The necessity to match the PDF of slopes and the spectrum was noted in paper [9].

[15] We are grateful to [10] who supplied us with the program for numerically calculating the spectrum.

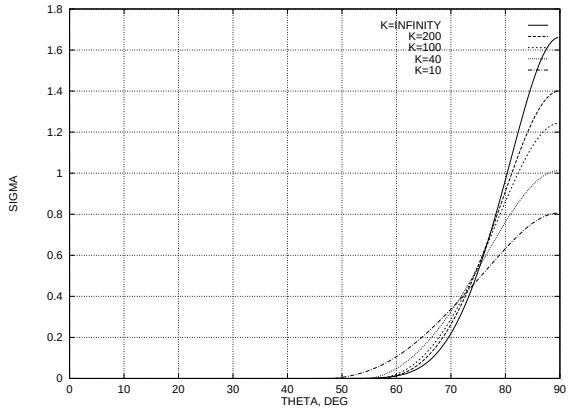

Figure 4. Backscattering cross section as a function of the grazing incident angle θ for different values of k.

elevations $D(r,\psi)$. The function $D(r,\psi)$ was calculated by the formula (161) on the basis of the spectrum published in [10]. Special attention was paid to such approximation of the function $D(r,\psi)$, which provides the correct value of the second derivatives in the point $r=0$, the correct values of $\langle\gamma_1^2\rangle$ and $\langle\gamma_2^2\rangle$. In this case the results of the Kirchhoff approximation match the limiting case of the GO approximation given by the formula (150).

In Figure 4 we present the results of calculations of the radar cross section as a function of the grazing incident angle θ for different values of k. We used the anisotropic 2-D spectrum of wind-driven waves taken from [10] for the wind speed $u = 10m \cdot s^{-1}$ and the Cox-Munk PDF of slopes for the same wind speed.

To estimate how the Cox-Munk PDF influences the scattering cross section, we performed the calculations for the same anisotropic spectrum of surface waves, but used the Gaussian PDF of slopes. The results are presented in Figure 5.

In the region of small grazing angles both Cox-Munk and Gaussian cross sections became very small. To eliminate the possible influence of computational errors on the results in this region, we present in Figure 6 the results obtained in the GO approximation, $k=\infty$, when we can use analytical formula (150).

The same result is presented in Figure 6 in the logarithmic scale where the ratio of the Cox-Munk and the Gaussian cases is clearer in the region of small grazing angles.

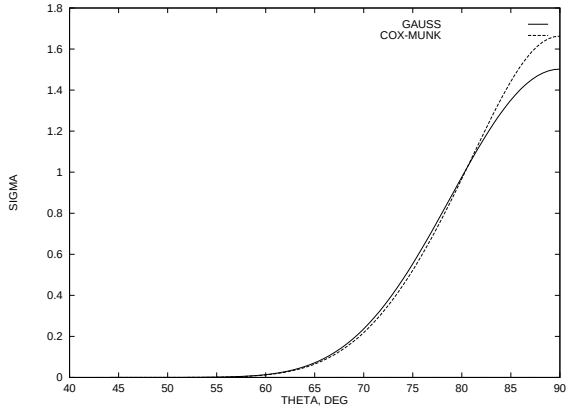

Figure 5. Angular dependence of the backscattering cross section for Cox-Munk and for Gaussian approximation of PDF in the geometric optics limit ($k = \infty$).

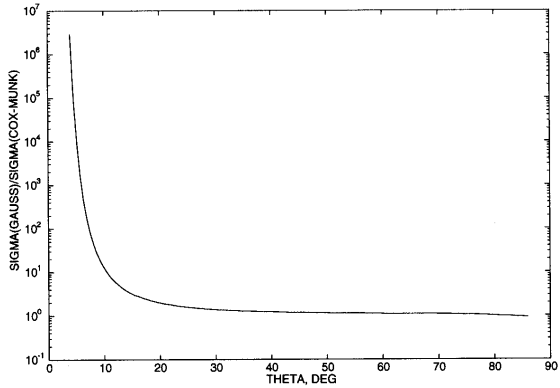

Figure 6. The ratio of the backscattering cross sections for Gaussian and Cox-Munk cases in the limit of geometrical optics ($k = \infty$).

Similar results were obtained for the finite values of the wavenumber. In Figure 7 we present the angular dependence of the radar cross section for $k = 30m^{-1}$ for the Cox-Munk and the Gaussian PDF of slopes.

In Figure 8 we present the radar cross section as a function of the azimuthal angle. Both the anisotropy of the spectrum and anisotropy of the PDF affect this angular dependence in the case of the finite k (i.e., in the Kirchhoff approximation). The difference between the curves

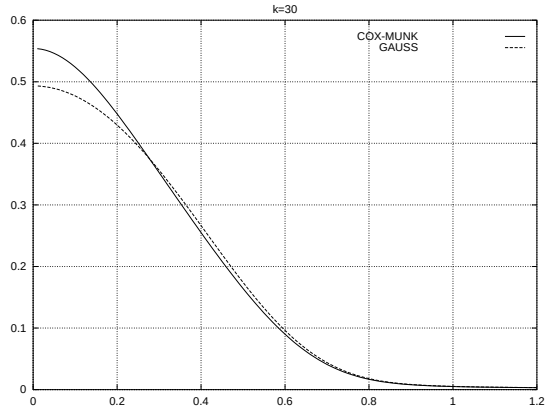

Figure 7. The radar cross section as a function of the incident angle $\alpha = 90^o - \theta$ for $k = 30\ m^{-1}$, $kh = 16.5$. Similar to the geometric optic limit, the Gaussian approximation reduces the radar cross section in the region near the nadir and increases it in the region of small grazing angles.

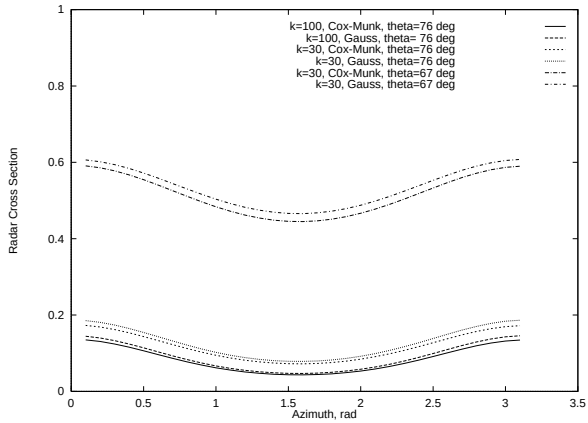

Figure 8. Azimuthal dependence of the radar cross section for the wind speed $u_{10} = 10$ m/s for different values of k and different grazing angles θ.

corresponding to the Cox-Munk and the Gaussian PDF is caused by the anisotropy of the PDF. In the case of the GO limit, only the anisotropy of the PDF is important.

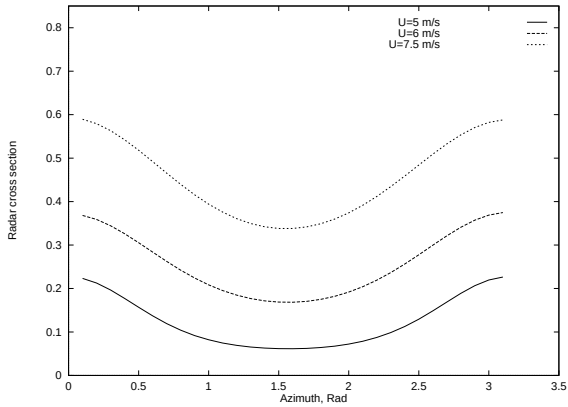

Figure 9. Azimuthal dependence of radar cross section for $k = 30\,\mathrm{m}^{-1}$, $\theta = 76^o$, and different wind speeds U, m/s.

Experimental data on the azimuthal dependence of the radar cross section (see, e.g., [11–13] are in qualitative agreement with the results presented in Figure 8.[16]

We studied how the wind speed affects the azimuthal dependence of the radar cross section. In Figure 9 we present the set of curves showing the azimuthal dependence of the radar cross section for different wind speeds.

It is clear from these curves that the lower return corresponds to the lower wind speed. But the ratio $\Sigma_{\mathrm{Upwind}}/\Sigma_{\mathrm{Cross-wind}}$ of radar cross sections in upwind and in cross-wind directions strongly depends on the wind speeds and is larger for low wind speed than for relatively large ones. This ratio is presented in Figure 10. It follows from this plot that measuring the ratio $\Sigma_{\mathrm{Upwind}}/\Sigma_{\mathrm{Cross-wind}}$, which is independent of the radar calibration, we can obtain information concerning wind speed. Fortunately, in the region of low wind speed (and lower radar return) the sensitivity of this ratio to wind speed increases.

[16] The measurements described in [11–13] were performed in the range of Bragg scattering. Because of this, we cannot expect quantitative agreement of these results with the results of the calculations we performed in the Kirchhoff approximation (for much larger values of k).

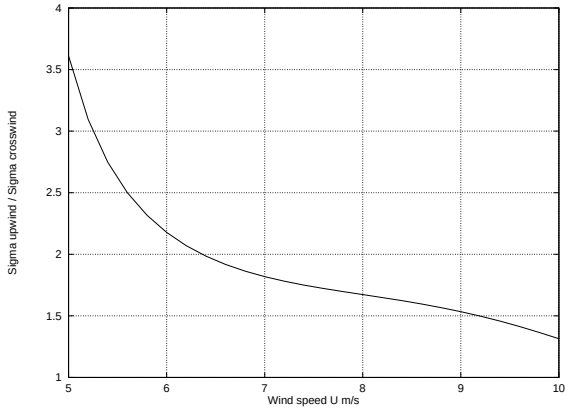

Figure 10. The ratio of scattering cross section in upwind and crosswind direction versus wind speed for $k = 30\,\mathrm{m}^{-1}$.

12. SUMMARY

The main results of this paper are as follows:

1. The only statistical characteristics necessary to describe the scattering cross section are joint PDF or joint CF for *differences* in elevation at several points of the random surface.

2. For the mathematical description of the multivariate non-Gaussian probability distributions we used a decomposition of an arbitrary PDF in the sum of an auxiliary Gaussian PDF having different parameters. This method can successfully replace the standard representation of non-Gaussian distributions in terms of the Edgeworth or Gram-Charlier series and is free from the main disadvantage of these approaches, i.e., negative probabilities. This method is very simple in application and it easily allows one to find different mean values as a sum of corresponding partial Gaussian mean values.

3. We obtained the multivariate characteristic function for an arbitrary number of differences in elevation of a random surface. The corresponding probability distribution satisfies the following conditions: (a) the spectrum (or correlation function) of surface is the given (anisotropic) function, and (b) the joint probability distribution of two principal slopes of the surface is the given (anisotropic) function.

4. We used the generalized experimental data for the spectrum of the sea surface from paper [10], and the data for joint PDF of slopes from papers [2, 3] for the wind speed $10\,m \cdot s^{-1}$.

5. We calculated the scattering cross sections for the absolutely reflecting air-sea interface in the Kirchhoff approximation for the Gaussian and non-Gaussian (Cox-Munk) joint PDF of slopes, and found a significant difference between these two cases, especially in the range of small grazing angles.

6. We obtained the universal angular dependence of the variance of slope for the case in which the spectrum is symmetrical with respect to some direction (in our case wind direction). This result agrees well with the experimental data; it follows only from the symmetry of spectrum and does not depend on the probability distribution (see Appendix A).

ACKNOWLEDGMENT

This document has been generated as part of a joint NOAA/DOD–Advanced Sensor Application Program.

APPENDIX A. ANGULAR DEPENDENCE OF THE VARIANCE OF SLOPE

The slope of a surface at a point $\mathbf{r}$ in a direction determined by the unit vector $\mathbf{n}$, is given by the formula

$$\gamma(\mathbf{n}, \mathbf{r}) \equiv \mathbf{n}\nabla\zeta(\mathbf{r}). \tag{154}$$

We assume that the spectrum of surface $\Phi(\mathbf{q})$ is symmetrical with respect to wind direction, determined by the unit vector $\mathbf{m}_1$. If we choose the x-axis along the vector $\mathbf{m}$, we obtain

$$\mathbf{m}_1 = (1, 0); \quad \mathbf{q} = (q\cos\varphi, q\sin\varphi), \tag{155}$$

where φ is the angle between $\mathbf{q}$ and the wind direction. The symmetry of the spectrum with respect to the wind direction means that

$$\Phi(q, \varphi) = \Phi(q, -\varphi). \tag{156}$$

The structure function of the surface in terms of the spectrum Φ has the form (see (55))

$$D(r, \psi) = 2\iint [1 - \cos(\mathbf{qr})]\,\Phi(q, \varphi)\, qdqd\varphi, \tag{157}$$

where $\mathbf{r} = \mathbf{r}' - \mathbf{r}'' = \mathbf{n}r$. We present the vector $\mathbf{r}$ in the form

$$\mathbf{r} = \mathbf{n}r; \quad \mathbf{n} = (\cos\psi, \sin\psi), \tag{158}$$

where ψ is the angle between $\mathbf{r}$ and the wind direction. For the scalar product $\mathbf{qr}$, entering in (157), we have

$$\mathbf{qr} = qr\cos(\varphi - \psi). \tag{159}$$

Using the known formula [14], **8.511.**4,

$$\cos[qr\cos(\varphi - \psi)] = J_0(qr) + 2\sum_{n=1}^{\infty}(-1)^n J_{2n}(qr)\cos(2n\varphi - 2n\psi), \tag{160}$$

we obtain for $D(r,\psi)$:

$$\begin{aligned} D(r,\psi) = D(\mathbf{r}) = 2\int_0^{\infty}[1 - J_0(qr)]\,qdq\int_0^{2\pi}\Phi(q,\varphi)\,d\varphi \\ - 4\sum_{n=1}^{\infty}(-1)^n\int_0^{\infty}J_{2n}(qr)\,qdq\int_0^{2\pi}\Phi(q,\varphi)\cos(2n\varphi - 2n\psi)\,d\varphi. \end{aligned} \tag{161}$$

The slope of the surface, taken in the direction $\mathbf{n}$, according to (154) can be presented in the form

$$\gamma(\mathbf{r},\mathbf{n}) = \lim_{l\to 0}\frac{\zeta(\mathbf{r}+\mathbf{n}l) - \zeta(\mathbf{r})}{l}. \tag{162}$$

$$\left\langle\gamma^2(\mathbf{r},\mathbf{n})\right\rangle = \lim_{l\to 0}\frac{\left\langle[\zeta(\mathbf{r}+\mathbf{n}l) - \zeta(\mathbf{r})]^2\right\rangle}{l^2} = \lim_{l\to 0}\frac{D(\mathbf{n}l)}{l^2}, \tag{163}$$

where $\mathbf{n}l$, the argument of the structure function, is equal to $(l\cos\psi, l\sin\psi)$. If we substitute (161) in (163) and set $r = l \to 0$, the known limits

$$\begin{aligned} &\lim_{l\to 0}\frac{1 - J_0(ql)}{l^2} = \frac{q^2}{4}, \quad \lim_{l\to 0}\frac{J_2(ql)}{l^2} = \frac{q^2}{8}, \\ &\text{and } \lim_{l\to 0}\frac{J_{2n}(ql)}{l^2} = 0, \quad n = 2,3,... \end{aligned} \tag{164}$$

appear.

Therefore, only two beginning terms of expansion survive, while $l \to 0$ and the result is

$$\lim_{l\to 0} \frac{D(l,\psi)}{l^2} = \frac{1}{2}\int q^3 dq \int \Phi(q,\varphi)\, d\varphi + \frac{1}{2}\int q^3 dq \int \Phi(q,\varphi)\cos(2\varphi - 2\psi)\, d\varphi. \tag{165}$$

But

$$\cos(2\varphi - 2\psi) = \cos(2\varphi)\cos(2\psi) + \sin(2\varphi)\sin(2\psi), \tag{166}$$

and after integration over φ in (165) the term containing $\sin(2\varphi)$ vanishes because of $\Phi(q,\varphi) = \Phi(q,-\varphi)$. Thus, the general result is

$$\begin{aligned} \left\langle \gamma^2(\psi) \right\rangle &= \lim_{l\to 0} \frac{D(l,\psi)}{l^2} \\ &= \frac{1}{2}\int q^3 dq \int \Phi(q,\varphi)\, d\varphi \\ &\quad + \frac{1}{2}\cos(2\psi)\int q^3 dq \int \Phi(q,\varphi)\cos(2\varphi)\, d\varphi \\ &= a + b\cos(2\psi), \end{aligned} \tag{167}$$

where

$$a = \frac{1}{2}\int q^3 dq \int \Phi(q,\varphi)\, d\varphi, \quad b = \frac{1}{2}\int q^3 dq \int \Phi(q,\varphi)\cos(2\varphi)\, d\varphi. \tag{168}$$

If we substitute in (167)

$$\cos 2\psi = \cos^2\psi - \sin^2\psi,$$

we obtain

$$\left\langle \gamma^2(\psi) \right\rangle = A\cos^2\psi + B\sin^2\psi, \tag{169}$$

where

$$\begin{aligned} A &= a + b = \int_0^\infty q^3 dq \int_0^{2\pi} \Phi(q,\varphi)\cos^2\varphi d\varphi \geq 0, \\ B &= a - b = \int_0^\infty q^3 dq \int_0^{2\pi} \Phi(q,\varphi)\sin^2\varphi d\varphi \geq 0. \end{aligned} \tag{170}$$

If we set $\psi = 0$ in (169), we obtain the variance of the slope in the upwind direction:

$$\left\langle \gamma^2 (0) \right\rangle \equiv \left\langle \gamma_1^2 \right\rangle = A. \tag{171}$$

If we set $\psi = \pi/2$ in (169), we obtain the variance of the slope in the cross-wind direction:

$$\left\langle \gamma^2 (\pi/2) \right\rangle \equiv \left\langle \gamma_2^2 \right\rangle = B. \tag{172}$$

Therefore, formula (169) can be presented as follows:

$$\left\langle \gamma^2 (\psi) \right\rangle = \left\langle \gamma_1^2 \right\rangle \cos^2 \psi + \left\langle \gamma_2^2 \right\rangle \sin^2 \psi. \tag{173}$$

From (154) we find that the random value of the slope can be presented in the form

$$\gamma (\mathbf{n}, \mathbf{r}) = \gamma (\mathbf{r}, \psi) = \gamma_1 \cos \psi + \gamma_2 \sin \psi, \tag{174}$$

where

$$\gamma_1 = \frac{\partial \zeta (\mathbf{r})}{\partial x}, \quad \gamma_2 = \frac{\partial \zeta (\mathbf{r})}{\partial y} \tag{175}$$

are the random values of the slopes in the two principal (upwind and cross-wind) directions. If we calculate the mean square of (174), we obtain

$$\left\langle \gamma^2 (\psi) \right\rangle = \left\langle \gamma_1^2 \right\rangle \cos^2 \psi + + \left\langle \gamma_2^2 \right\rangle \cos^2 \psi + 2 \left\langle \gamma_1 \gamma_2 \right\rangle \sin \psi \cos \psi. \tag{176}$$

From comparison of this formula with (173) we find that

$$\left\langle \gamma_1 \gamma_2 \right\rangle \equiv 0. \tag{177}$$

We emphasize that the main results of Appendix A, formulae (173) and (177), are the precise consequences of the symmetry of the spectrum (156) and do not depend on the PDF of the surface. The symmetry condition is enough to derive these formulae.

Note that the angular dependence of the form (167) was widely used in many experimental works.

REFERENCES

1. Tatarskii, V. I., "Formulation of rough-surface scattering theory in terms of phase factors and approximate solutions based on this formulation," *Waves in Random Media,* Vol. 7, 557–578, 1997.

2. Cox, C., and W. Munk, "Statistics of the sea surface derived from sun glitter," *J. Mar. Res.,* Vol. 13, 198–227, 1954.
3. Cox, C., and W. Munk, "Measurement of the roughness of the sea surface from photographs of the sun's glitter," *J. Opt. Soc. Am.,* Vol. 44, No. 11, 838–850, 1954.
4. Metropolis, N., M. Rosenbluth, A. Teller, and E. Teller, *Journal of Chemical Physics,* Vol. 21, 1087–1092, 1953. See also Press, W. H., S. A. Teukolsky, W. T. Vettering, and B. P. Flannery, *Numerical Recipes in C,* Section 10.9, Cambridge University Press, 1997.
5. Bock, E. J., and T. Hara, "Optical measurements of capillary-gravity wave spectra using a scanning laser slope gauge," *J. Atmos. Ocean. Technol.,* Vol. 12, No. 2, 395–403, 1995.
6. Shaw, J. A., and J. H. Churnside, "Scanning-laser glint measurements of sea-surface slope statistics," *Appl. Opt.,* Vol. 36, No. 18, 4202–4213, 1997.
7. Tatarskii, V. V., and V. I. Tatarskii, "Non-Gaussian statistical model of the ocean surface for wave-scattering theories," *Waves in Random Media,* Vol. 6, 419–435, 1996.
8. Apel, J. R., "An improved model of the ocean surface wave vector spectrum and its effects on radar backscatter," *J. Geophys. Res.,* Vol. 99, 16,269–16,291, 1994.
9. Nickolaev, N. I., O. I. Yordanov, and M. A. Michalev, "Non-Gaussian effects in two-scale model for rough surface scattering," *Journal Geophys. Res.,* Vol. 97, No. C10, 15.617–15.624, 1992.
10. Elfouhaily, T., B. Chapton, K. Katsaros, and D. Vandemark, "A unified directional spectrum for long and short wind-driven waves," *J. Geophys. Res.,* Vol. 102, No. C7, 15,781–15,796, 1997.
11. Jones, W. L., and L. C. Schroeder, "Radar backscatter from the ocean: dependence on surface friction velocity," *Boundary-Layer Meteorol.,* Vol. 13, 133–149, 1978.
12. Schroeder, L. C., P. R. Schaffner, J. L. Mitchell, and W. L. Jones, "AAFE RADSCAT 13.9 GHz measurements and analysis: wind-speed signature of the ocean," *IEEE J. Oceanic Eng.,* Vol. 10, No. 4, 346–357, 1985.
13. Masuko, H., K. Okamoto, M. Shimada, and S. Niwa, "Measurement of microwave signatures of the ocean surface using X and Ka band airborne scatterometers," *J. Geophys. Res.,* Vol. 91, No. C11, 13,065–13,083, 1986.
14. Gradshteyn, I. S., and I. M. Ryzhik, *Table of Integrals, Series, and Products,* Corrected and enlarged ed. prepared by A. Jeffrey, Academic Press, Inc., San Diego, CA., 1980.